Hybrid Mechanistic Data-Driven Modeling for the Deterministic Global Optimization of a Transcritical Organic Rankine Cycle

Wolfgang R. Huster[a] , Artur M. Schweidtmann[a] and Alexander Mitsos[b,a,c*]

[a]*Process Systems Engineering (AVT.SVT), RWTH Aachen University, 52074 Aachen, Germany*
[b]*JARA - ENERGY, 52056 Aachen, Germany*
[c]*Institute of Energy and Climate Research: Energy Systems Engineering (IEK-10), Forschungszentrum Jülich GmbH, Wilhelm-Johnen-Straße, 52425 Jülich, Germany*
amitsos@alum.mit.edu

Abstract

Global optimization is desirable for the design of chemical and energy processes as design decisions have a significant influence on the economics. A relevant challenge for global flowsheet optimization is the incorporation of accurate thermodynamic models. A promising alternative to conventional thermodynamic property models is the integration of data-driven surrogate models into mechanistic process models and deterministic global optimization in a reduced space. In our previous works, we trained artificial neural networks (ANNs) on thermodynamic data and included the surrogate models in the global flowsheet optimization of subcritical organic Rankine cycles (ORC). In this work, we extend the framework to the optimization of transcritical ORCs operating at a supercritical high pressure level and subcritical low pressure level. We train separate ANNs for supercritical and subcritical thermodynamic properties. ANNs with a small number of neurons can learn the thermodynamic properties to sufficient accuracy. We identify the optimal working fluid among 122 available fluids in the thermodynamic library CoolProp via a deterministic global optimization of the hybrid process model using the solver MAiNGO. The results show that the process can be optimized efficiently and that transcritical operation can enable high power generation.

Keywords: Surrogate model, Artificial neural networks, MAiNGO, Geothermal power, Supercritical properties

1. Introduction

Numerical optimization of the design and operation of energy processes using renewable energy resources is a key element for the transition to a carbon neutral economy. Making use of low-temperature power resources, such as geothermal brine, will become a relevant part of future power generation. However, the most relevant processes for this energy transformation, organic Rankine cycles (ORCs), often suffer from low thermal efficiencies. This is, among other effects, caused by the isothermal evaporation of the working fluid (WF), which results in high exergy destruction. One way to circumvent is the evaporation at supercritical pressure, i.e., at a pressure level higher than the critical pressure of the working fluid p_c. Fluids at supercritical pressure levels exhibit different thermodynamic properties than at subcritical pressure.

Supercritical pressure levels in ORCs have been investigated in many studies (Chen et al., 2006; Schuster et al., 2010; Gao et al., 2012). Most authors perform a variation of

process parameters to improve the performance (Shengjun et al., 2011; Yağlı et al., 2016; Xu et al., 2016) or apply a local optimization solver (Le et al., 2014; Maraver et al., 2014). Although rare, experimental investigations validated the potential advantages of operating ORCs at supercritical pressure (Kosmadakis et al., 2016). A review on transcritical ORC studies, experimental data, and existing plants is given by Lecompte et al. (2019).

In our previous works (Schweidtmann et al., 2018; Huster et al., 2019a,b), we investigated the deterministic global optimization of ORCs employing pure fluids at subcritical pressure levels. Solving the optimization problem in a reduced-space using our in-house solver MAiNGO (Bongartz et al., 2018), we were able to illustrate the benefit of using surrogate models for the calculation of accurate thermodynamic properties. For this, we train artificial neural networks (ANNs) on subcritical thermodynamic data, which allow for an explicit model formulation. Together with tighter relaxations compared to the original thermodynamic equations, this drastically reduces CPU times (Schweidtmann and Mitsos, 2019; Schweidtmann et al., 2018).

Surrogate models and ANNs have been discussed in engineering literature for decades (Wang, 2006; Himmelblau, 2000). Furthermore, ANNs have been employed for the prediction of supercritical fluid properties by several authors (Mehdizadeh and Movagharnejad, 2011; Eslamimanesh et al., 2011). Arslan and Yetik (2011) and Rashidi et al. (2011) used ANNs to learn ORC process models in a black-box approach and optimized these. The novelty of this work compared to earlier works is that ANNs have not been used for learning supercritical fluid properties and subsequently used in a hybrid model that is to be optimized to guaranteed global optimality. In this work, we apply ANNs for the prediction of supercritical fluid properties within an ORC process optimization. Further, we select the most promising fluid candidates among a wide range of fluids available in the thermodynamic library CoolProp (Bell et al., 2014).

2. ORC process model

We adopt the geothermal set up presented in (Huster et al., 2019a) and adjust the model to transcritical operation. Figure 1 shows the ORC flowsheet, indicating the super- and subcritical pressure levels. The models of the pump, expander and condenser are identical to (Huster et al., 2019a). We model the evaporator as a single process unit due to the continuous phase change and assume a constant heat transfer coefficient. The supercritical phase change requires constraining the minimum temperature difference along the heat transfer, similar to the use of WF mixtures (Huster et al., 2020). For this, the evaporator is discretized along its length. In each discretization cell, we introduce an inequality on the minimum temperature difference to avoid unphysical temperature crossover. When choosing ten cells or less in the process optimization, temperature crossovers occurred at the optimal solution point, resulting in a relaxed solution. To ensure sufficient temperature difference for all WF candidates, we choose 50 cells in all further optimizations. We found that the influence of cell number on the CPU time of the process optimization is almost linear between 10 and 100 cells, ranging from 95 to 632 s. This is summed over six cores that are used for the parallelized branch-and-bound algorithm. Further, we ensure that the expansion process does not cross the two-phase region by setting a lower bound for the specific entropy at the outlet of the evaporator, as illustrated in Figure 2. For the lower bound of the high pressure level p_{HP}, we select $1.1 \cdot p_c$. This avoids pressure levels close to or below the critical point, which requires different models to account for the two-phase region.

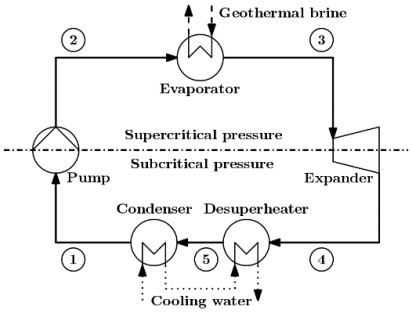

Figure 1: Flowsheet of the transcritical ORC. The circled numbers indicate fluid states. Above the dashed line, the process operates at supercritical pressure, below at subcritical pressure.

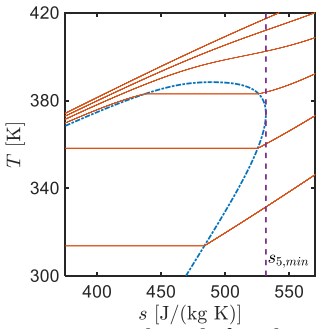

Figure 2: Lower bound for the minimum specific entropy of RC-318 (purple dashed line) for the superheated state at the expander inlet. Orange lines indicate isobars, the blue dash-dotted line indicates the two-phase region.

3. Method

CoolProp (Bell et al., 2014) provides accurate thermodynamic equations of state for 122 fluids. Many of these fluids are not suitable for the presented case study due to their thermodynamic properties. Thus, we only consider WF candidates that can be evaporated at supercritical pressure and condensed at the present conditions. We apply the following rigorous feasibility preselection criteria to all 122 fluids in CoolProp: critical temperature T_c < 400 K, saturation temperature at a pressure of 10 bar $T|^{sat}_{10\ \mathrm{bar}}$ > 260 K. For the preselected fluids, we perform an automated data generation using CoolProp, which we extend to transcritical properties. The procedure for subcritical properties is described in more detail in (Huster et al., 2019b). For supercritical properties, we generate 10^5 data points. We perform the ANN training in Matlab R2018b using the Bayesian backpropagation algorithm, 700 training epochs, and randomly split the data into 40% training data, 30% validation data, and 30% test data. In the training procedure, we minimize the mean-squared error (MSE) on the training data. We optimize the resulting hybrid model using our open-source deterministic global optimization solver MAiNGO (Bongartz et al., 2018).

4. Results

4.1. Artificial neural network accuracy

Table 1 shows that ANNs can learn temperature *T* as a function of pressure *p* and mass-specific enthalpy *h* in the supercritical region with high accuracy. Based on these results and desirable accuracy (Huster et al., 2019a), we select six neurons for both hidden layers for supercritical properties. For subcritical properties, we also select two hidden layers with six neurons each (Huster et al., 2019a,b).

Table 1: Mean-squared errors of the ANNs on the training data for the supercritical region, in dependence of the number of neurons in both hidden layers (input variables: *p*, *h*; output variable: *T*; fluid: RC318).

Number of neurons	5	6	7	8	9	10
MSE [K^2]	$5.3\cdot10^{-8}$	$6.0\cdot10^{-9}$	$6.1\cdot10^{-9}$	$1.1\cdot10^{-10}$	$4.7\cdot10^{-10}$	$1.4\cdot10^{-10}$

4.2. Process optimization results

The process optimization results of the five fluids with the highest net power generation P_{net} (Table 2) show that transcritical operation allows for much higher net power generation than using isobutane at subcritical conditions ($P_{net,max}$ = 16.5 MW, (Huster et al., 2019a)). However, no general claim can be made as we have not performed the WF selection procedure for subcritical operation for this case study. We give p^* as the ratio of high pressure level and critical pressure ($p^* = p_{HP}/p_c$), and the thermal efficiency η_{th}. Aside from high power generation in the turbine P_{turb}, high values of p_{HP} also strongly increase power consumption in the pump P_{pump} and investment costs *Inv* respectively levelized cost of electricity *LCOE*. The CPU times are between $2 \cdot 10^2$ and $2 \cdot 10^4$ s. Using six CPU cores, this corresponds to less than one hour of wall time. Five of the 21 preselected fluid candidates are infeasible.

Table 2: Results of the thermodynamic optimization for the five WF candidates with the highest P_{net}, sorted by decreasing P_{net}.

Fluid	$\dot{m}_{WF}$ [kg/s]	p_{HP} [bar]	p_{LP} [bar]	P_{net} [MW]	P_{pump} [MW]	η_{th} [%]	*Inv* [m US-$]	*LCOE* [US-$/MWh]	p^* [-]
R507A	17.2	65.2	15.8	25.5	10.3	9.1	51.4	57.3	1.8
R125	20.7	71.8	16.9	25.5	12.2	8.8	53.3	59.5	2.0
R143a	14.5	62.2	15.5	25.4	9.3	9.3	50.1	56.3	1.7
R404A	16.7	64.1	15.5	25.4	9.9	9.1	50.9	57.1	1.7
R227EA	20.9	31.9	5.8	25.3	5.0	9.2	46.0	52.1	1.1

The thermoeconomic optimization, i.e., minimization of *LCOE*, takes the investment cost of the process units into account. The results reflect the increased cost of operating at high pressure levels (Table 3). For four of the five given WF candidates, operating the ORC at $p^* = 1.1$ is economically favorable. As this is the lower bound for p_{HP} of each respective WF, the results suggest that subcritical operation could be the most economic option. The CPU times for the thermoeconomic optimizations are between $3 \cdot 10^2$ and $4 \cdot 10^4$ s, summed over all cores. Although the CPU times are higher compared to the thermodynamic optimization, they are still viable for process design.

Table 3: Results of the thermoeconomic optimization for the five WF candidates with the lowest *LCOE*, sorted by increasing *LCOE*.

Fluid	$\dot{m}_{WF}$ [kg/s]	p_{HP} [bar]	p_{LP} [bar]	P_{net} [MW]	P_{pump} [MW]	η_{th} [%]	*Inv* [m US-$]	*LCOE* [US-$/MWh]	p^* [-]
R227EA	19.9	31.9	6.2	24.6	4.7	9.4	44.2	51.5	1.1
R1234yf	14.1	36.8	9.0	23.4	4.6	9.5	43.0	52.6	1.1
Propylene	5.7	49.6	14.8	22.5	5.0	10.1	42.8	54.4	1.1
R143a	13.5	55.6	16.1	25.0	7.4	9.3	47.8	54.8	1.5
n-Propane	5.4	46.3	12.3	21.7	4.8	10.3	41.6	54.8	1.1

The *T*-*Q*-plots for the best-performing WFs of the thermodynamic and thermoeconomic optimization are given in Figure 3. For $P_{net,max}$, the temperature curve is almost parallel along the evaporator, which comes close to minimum exergy destruction. This is not the case for $LCOE_{min}$, and higher temperature differences between heat source and WF occur. Like this, the HX investment cost is reduced due to the decreased area and a smaller pressure factor.

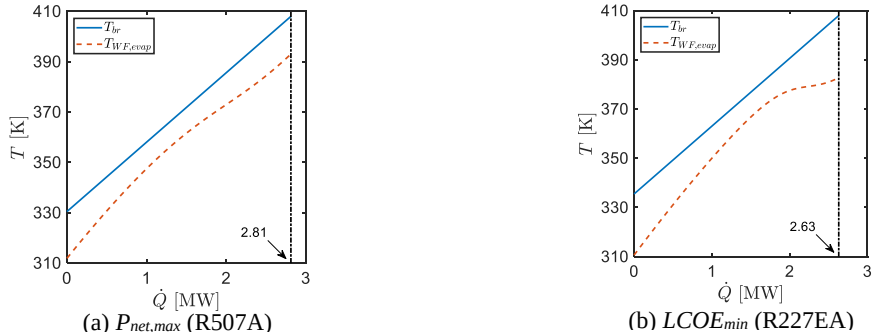

(a) $P_{net,max}$ (R507A) (b) $LCOE_{min}$ (R227EA)

Figure 3: *T-Q*-plots for the WFs with the highest net power (R507A) and lowest *LCOE* (R227EA), illustrating the temperatures of the geothermal brine T_{br} and WF in the evaporation $T_{WF,evap}$.

5. Conclusion and outlook

We propose an approach for globally optimal WF selection and process design for transcritical ORCs. For this, we train ANNs on accurate supercritical thermodynamic data and subsequently integrate them into a mechanistic process model. We solve the resulting hybrid model using the deterministic global solver MAiNGO. We identify the optimal WF among 122 fluids that are available in CoolProp.

We show that ANNs with a small number of neurons (two hidden layers with six neurons each) can learn supercritical data with high accuracy, which is comparable to subcritical data. The thermodynamic optimization reveals the potential of operating ORC at supercritical pressure levels. The nonisothermal evaporation allows to adjust the slope of the evaporation curve towards the heat source, approaching minimal exergy destruction in the evaporation. In contrast, the thermoeconomic optimization can lower investment costs significantly for similar net power generation. All optimizations can be solved to global optimality within less than two hours of wall time using six CPU cores. This demonstrates the viability of the proposed approach.

Future work includes the optimization of more detailed models with heat transfer correlations embedded. It would further be relevant to take the influence of fluid stability at high pressure levels and environmental fluid properties into account.

Acknowledgments: The authors gratefully acknowledge the financial support of the Kopernikus project SynErgie by the Federal Ministry of Education and Research (BMBF) and the project supervision by the project management organization Projektträger Jülich (PtJ).

References

Arslan, O., Yetik, O., 2011. ANN based optimization of supercritical ORC-binary geothermal power plant: Simav case study. Applied Thermal Engineering 31 (17-18), 3922-3928.

Bell, I. H., Wronski, J., Quoilin, S., Lemort, V., 2014. Pure and pseudo-pure fluid thermophysical property evaluation and the open-source thermophysical property library CoolProp. Industrial & Engineering Chemistry Research 53 (6), 2498-2508.

Bongartz, D., Najman, J., Sass, S., Mitsos, A., 2018. MAiNGO - McCormick-based Algorithm for mixed-integer Nonlinear Global Optimization. Tech. rep., Process Systems Engineering (AVT.SVT), RWTH Aachen University.

Chen, Y., Lundqvist, P., Johansson, A., Platell, P., 2006. A comparative study of the carbon dioxide transcritical power cycle compared with an organic Rankine cycle with R123 as working fluid in waste heat recovery. Applied Thermal Engineering 26 (17-18), 2142-2147.

Eslamimanesh, A., Gharagheizi, F., Mohammadi, A. H., Richon, D., 2011. Artificial neural network modeling of solubility of supercritical carbon dioxide in 24 commonly used ionic liquids. Chemical Engineering Science 66 (13), 3039-3044.

Gao, H., Liu, C., He, C., Xu, X., Wu, S., Li, Y., 2012. Performance analysis and working fluid selection of a supercritical organic Rankine cycle for low grade waste heat recovery. Energies 5 (9), 3233-3247.

Himmelblau, D. M., 2000. Applications of artificial neural networks in chemical engineering. Korean journal of chemical engineering, *17*(4), 373-392.

Huster, W. R., Schweidtmann, A. M., Mitsos, A., 2019a. Impact of accurate working fluid properties on the globally optimal design of an organic Rankine cycle. Computer Aided Chemical Engineering 47, 427-432.

Huster, W. R., Schweidtmann, A. M., Mitsos, A., 2019b. Working fluid selection for organic Rankine cycles via deterministic global optimization of design and operation. Optimization and Engineering, in press.

Huster, W. R., Schweidtmann, A. M., Mitsos, A., 2020. Globally optimal working fluid mixture composition for geothermal power cycles, submitted September 6th, 2019.

Kosmadakis, G., Manolakos, D., Papadakis, G., 2016. Experimental investigation of a low-temperature organic Rankine cycle (ORC) engine under variable heat input operating at both subcritical and supercritical conditions. Applied Thermal Engineering 92, 1-7.

Le, V. L., Feidt, M., Kheiri, A., Pelloux-Prayer, S., 2014. Performance optimization of low-temperature power generation by supercritical ORCs (organic Rankine cycles) using low GWP (global warming potential) working fluids. Energy 67, 513-526.

Lecompte, S., Ntavou, E., Tchanche, B., Kosmadakis, G., Pillai, A., Manolakos, D., Paepe, M. D., 2019. Review of experimental research on supercritical and transcritical thermodynamic cycles designed for heat recovery application. Applied Sciences 9 (12), 2571.

Maraver, D., Royo, J., Lemort, V., Quoilin, S., 2014. Systematic optimization of subcritical and transcritical organic Rankine cycles (ORCs) constrained by technical parameters in multiple applications. Applied Energy 117, 11-29.

Mehdizadeh, B., Movagharnejad, K., 2011. A comparison between neural network method and semi empirical equations to predict the solubility of different compounds in supercritical carbon dioxide. Fluid Phase Equilibria 303 (1),40-44.

Rashidi, M. M., Bég, O. A., Parsa, A. B., Nazari, F., 2011. Analysis and optimization of a transcritical power cycle with regenerator using artificial neural networks and genetic algorithms. Proceedings of the Institution of Mechanical Engineers, Part A: Journal of Power and Energy 225 (6), 701-717.

Schuster, A., Karellas, S., Aumann, R., 2010. Efficiency optimization potential in supercritical organic Rankine cycles. Energy 35 (2), 1033-1039.

Schweidtmann, A. M., Huster, W. R., Lüthje, J. T., Mitsos, A., 2018. Deterministic global process optimization: Accurate (single-species) properties via artificial neural networks. Computers & Chemical Engineering 121, 67-74.

Schweidtmann, A. M., Mitsos, A., 2019. Deterministic global optimization with artificial neural networks embedded. Journal of Optimization Theory and Applications 180 (3), 925-948.

Shengjun, Z., Huaixin, W., Tao, G., 2011. Performance comparison and parametric optimization of subcritical organic Rankine cycle (ORC) and transcritical power cycle system for low-temperature geothermal power generation. Applied Energy 88 (8), 2740-2754.

Wang, G. G., Shan, S., 2006. Review of metamodeling techniques in support of engineering design optimization. Journal of Mechanical Design 129, 370-380.

Xu, H., Gao, N., Zhu, T., 2016. Investigation on the fluid selection and evaporation parametric optimization for sub- and supercritical organic Rankine cycle. Energy 96, 59-68.

Yağlı, H., Koç, Y., Koç, A., Görgülü, A., Tandiroğlu, A., 2016. Parametric optimization and exergetic analysis comparison of subcritical and supercritical organic Rankine cycle (ORC) for biogas fuelled combined heat and power (CHP) engine exhaust gas waste heat. Energy 111, 923-932.